Ray-Tracing based Validation of Spatial Consistency for Geometry-Based Stochastic Channels

Fjolla Ademaj*§, Stefan Schwarz*§, Ke Guan‡, Markus Rupp§

*Christian Doppler Laboratory for Dependable Wireless Connectivity for the Society in Motion
§ TU Wien, Institute of Telecommunications, Gusshausstrasse 25/389, A-1040 Vienna, Austria
‡State Key Laboratory of Rail Traffic Control and Safety, Beijing Jiaotong University, 100044, Beijing, China
Email: {fademaj, sschwarz, mrupp}@nt.tuwien.ac.at, kguan@bjtu.edu.cn

***Abstract*—For real-world performance evaluation, channel models should be accurate in reflecting a realistic behavior between transmitter and receiver. A major concern with the actual standardized channel models, is that they do not consider the time evolution and are relevant only for drop based simulations. The need for spatial consistency of these channel models has been also acknowledged by standardization bodies, e.g., 3GPP, and alternative models are under discussion. In this paper, we compare the statistics generated with the 3GPP 3D channel model to those of ray tracing simulations and validate our method to achieve spatial consistency. Moreover, we estimate the correlation parameters such that the results obtained with our method match the ray-tracing results.**

***Index Terms*—Spatial Correlation, 3GPP 3D channel model, Ray-tracing, Circular correlation, Directional data**

I. Introduction

Developing channel models that reflect the realistic behavior between transmitter and receiver is a crucial issue in evaluating the performance of various techniques in wireless communications. The advanced 5G techniques such as FD-MIMO and 3-dimensional (3D) beamforming, require the use of a channel model that encompasses the main characteristics of large antenna arrays such as the angular spread in both azimuth and elevation, thus characterizing the propagation environment in three dimensions [1, 2]. This channel model is known as geometry-based stochastic channel (GSC) model and is adopted by standardization bodies such as the 3rd Generation Partnership Project (3GPP), IEEE or International Telecommunications Union (ITU). In terms of modeling, the GSC model can be seen as a balance between the two extremes of purely stochastic and purely deterministic channel modeling. The geometric modeling of the GSC channel consists of propagation parameters and antenna parameters, whereas the stochastic modeling enables to determine multipath-specific parameters such as delays, powers and angles of arrival- and departure [3]. In this way, the location of scatterers is not explicitly specified, only the direction of the multipaths generated from scattering objects.

This work has been funded by the Christian Laboratory for Dependable Wireless Connectivity for the Society in Motion. The financial support by the Austrian Federal Ministry of Science, Research and Economy and the National Foundation for Research, Technology and Development is gratefully acknowledged.

When used to evaluate the performance in large scenarios, comprising of many base stations and users, this model fails to give an accurate evaluation, i.e., in terms of beamforming, user separability, multiuser multiple input multiple output (MIMO) etc., since the propagation characteristics of two closely spaced user positions are uncorrelated. The lack of spatial correlation comes from the fact that in the 3GPP GSC models, the small scale parameters (e.g., path delays, powers, and arrival- and departure angles) are selected randomly according to tabulated distributions. In other words, for two users almost at the same position, scattering environment appears to be completely different, resulting in no common scatterers for thsee two user locations. There are a few channel models that introduce spatial correlation for GSC channel models such as COST2100 [4] and Wireless World Initiative New Radio (WINNER) [5]. In the COST2100 a global set of scatteres is shared by all users, whereas a different approach is introduced in the WINNER, where scatterers are progressively faded and new scatterers are shown up. This approach recently has been resolved in the quasi deterministic radio channel generator (QuaDRiGa) channel model [6]. The need for spatial consistency has been also acknowledged by standardization bodies e.g., 3GPP, and alternatives to extend the GSC channel models are provided in the recent 3GPP Technical Report TR38901.

In our previous work in [7, Sec.IV], we have extended the 3GPP 3D channel model [8, 9] by introducing a spatially consistent channel model. The model follows a stepwise procedure by first, generating independent and identically distributed (iid) random variables according to tabulated distributions used to introduce small scale parameters (see [7, Table I]), and second, interpolating between these random variables to get correlated variables for the actual user positions. The model uses a parameter known as *decorrelation distance*, which relates to the physical distance between users and represents the resolution of the iid random variables. Based on the value of decorrelation distance, the model gives different correlation levels. However, the decorrelation distance parameter was never parametrized and behaviour of the model in [7] was never validated, i.e., against measurements or ray-tracing simulations.

In this paper, in order to address the aforementioned issues

regarding spatial consistency for GSC channel models, we perform ray-tracing simulations to first validate the behaviour of our model proposed in [7]. Next, by comparing the statistics from ray-tracing simulations with the statistics of spatial correlation extension of the 3GPP GSC model, we provide a parametrization of the decorrelation distance parameter, referred as Δd from now on, based on hypothesis testing and the corresponding rejection rates.

II. System Model

We utilize a ray-tracing simulator [10, 11], which is already validated and calibrated against measurements. Since we are interested in the actual properties of the channel, i.e., normalized delay, azimuth of arrival (AoA), elevation of arrival (EoA), a ray-tracing tool is more useful, because these parameters are directly calculated based on the propagation characteristics. On the other side, when performing measurements, such parameters have to be estimated. The input to the ray-tracing simulator is a three-dimensional representation of the scenario as well as the relative permittivity of each of the elements in the scenario. As output, the ray-tracing gives several parameters that characterize propagation characteristics of the simulated environment, such as, angles of arrival- and departure in azimuth- and elevation, propagation delay and mulipath powers, pathloss, channel impulse response and channel transfer function [12].

We take advantage of the flexible modular structure of the ray-tracing simulator and simulate several urban environments, similar to the urban macro cell (UMa) scenario parametrized in 3GPP 3D model [8]. Figure 1 illustrates one example of an urban environment used in the ray-tracing simulator. The geometry of the scenario is chosen carefully to be in accordance with the 3GPP 3D-UMa scenario, i.e., average building height and average street width. Different material types, such as concrete, glass, brick, granite, metal, that are typical for urban environments, are considered in the model together with the electromagnetic properties of each material. Our goal is to observe the behaviour of AoA and EoA in terms of spatial consistency and understand how fast do these angular values change when changing the location. Considering a trace of consecutive spatial positions as illustrated in Figure 2, the AoA and EoA in arrival are measured in each position.

A. Correlation coefficient for circular distributions

When dealing with angular values, such as AoA and EoA, the usual statistics of sample mean and standard deviation cannot be used. Instead, for circular distribution, different statistical measures apply [13]. To determine the correlation between two circular variables ϕ_0 and ϕ_1, measured at two different spatial positions (x_0, y_0) and (x_1, y_1), respectively, the circular correlation coefficient formulates as,

$$r_j^{(\beta_m)} = \frac{\sum_{i=1}^{M} \sin\left(\phi_{i0} - \bar{\phi}_{i0}\right) \sin\left(\phi_{ij} - \bar{\phi}_{ij}\right)}{\sqrt{\sum_{i=1}^{M} \sin^2\left(\phi_{i0} - \bar{\phi}_{i0}\right)} \sqrt{\sum_{i=1}^{M} \sin^2\left(\phi_{ij} - \bar{\phi}_{ij}\right)}} \quad (1)$$

where $\bar{\phi}_{i0}$ is the mean direction of the first circular variable that repersents angular values measured always at the first position of the trace. The mean direction of the second circular variable corresponding to jth spatial position is denoted with $\bar{\phi}_{ij}$, where $j \in 1, 2, ..., J$ as indicated in Figure 2. To simplify the equation, we express the angular values of AoA and EoA with parameter ϕ. Variable M denotes the number of multipath components, while $\beta_m = \{\beta_1, \beta_2\}$ indicates the model under investigation, i.e., 3GPP 3D and ray-tracing, β_1 and β_2, respectively.

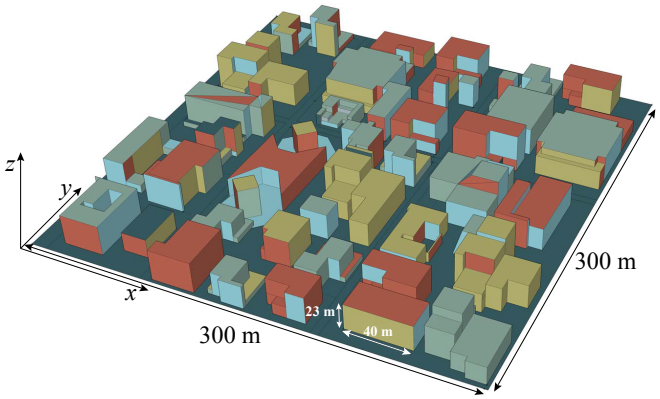

Fig. 1: Scenario example of an urban environment used in ray tracing simulations. Different materials are represented with different colors. The electromagnetic properties of each material for the corresponding frequency are considered in the ray-tracing.

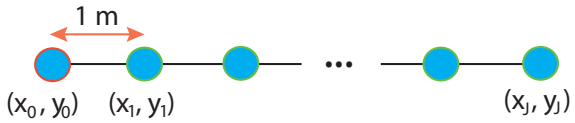

Fig. 2: Trace of consecutive spatial positions with a certain length evaluated at snapshots every one meter. The correlation is measured with respect to the initial spatial position at (x_0, y_0).

The mean direction $\bar{\phi}_{i0}$ is defined as,

$$\bar{\phi}_{i0} = \begin{cases} \tan^{-1}\left(\frac{\bar{P}}{\bar{Q}}\right), & \bar{P} > 0, \quad \bar{Q} > 0 \\ \tan^{-1}\left(\frac{\bar{P}}{\bar{Q}}\right) + \pi, & \bar{Q} < 0 \\ \tan^{-1}\left(\frac{\bar{P}}{\bar{Q}}\right) + 2\pi, & \bar{P} < 0, \quad \bar{Q} > 0 \end{cases} \quad (2)$$

with

$$\bar{P} = \sum_{i=1}^{M} \sin\left(\phi_{i0}\right) \quad (3)$$

and

$$\bar{Q} = \sum_{i=1}^{M} \cos\left(\phi_{i0}\right). \quad (4)$$

Similarly, the mean direction for other spatial positions, $\bar{\phi}_{ij}$ is calculated.

B. Binary hypothesis testing

The main goal of our method is to estimate the correlation coefficients for different values of decorrelation distance, Δd,

such that they are significantly the closest to the correlation coefficient produced by ray-tracing model. The correlation coefficient is denoted as $r_{j,k}^{(\beta_m)}$, where k represents the actual Δd used in the 3GPP 3D channel model with spatial consistency. We formulate this as a binary hypothesis problem of comparing the correlation coefficients of various Δds with that of ray tracing. The binary hypothesis is mathematically defined as,

$$\mathcal{H}_{0,k} : r_{j,k}^{(\beta_1)} = r_{j,0}^{(\beta_2)} \qquad \mathcal{H}_{1,k} : r_{j,k}^{(\beta_1)} \neq r_{j,0}^{(\beta_2)} \tag{5}$$

where $r_{j,k}^{(\beta_1)}$ and $r_{j,0}^{(\beta_2)}$ are correlation coefficients of 3GPP 3D model and ray-tracing, respectively. In order to comapare the sample correlation coefficients, we specifically use Fisher's z-transformation [14],

$$\mathrm{FT}\left(r_{j,k}^{(\beta_m)}\right) = \frac{1}{2}\ln\frac{1 + r_{j,k}^{(\beta_m)}}{1 - r_{j,k}^{(\beta_m)}} \tag{6}$$

where $\mathrm{FT}(\cdot)$ is the approximate variance-stabilizing transformation which transforms the respective $r_{j,k}^{(\beta)}$ to z-scores,

$$z = \frac{\mathrm{FT}\left(r_{j,k}^{(\beta_1)}\right) - \mathrm{FT}\left(r_{j,0}^{(\beta_2)}\right)}{\sqrt{\frac{1}{n_{\beta_1}-3} + \frac{1}{n_{\beta_2}-3}}} \tag{7}$$

where n_{β_1} and n_{β_2} are sample sizes of respective models. This transformation ensures to select the distance correlation from 3GPP 3D model $r_{j,k}^{(\beta_1)}$ which is the most similar with that of ray tracing $r_{j,0}^{(\beta_2)}$, while being sensitive to both variance and mean. This corresponds to finding the parameter under investigation, Δd, based on rejection rates of hypotheses. The evaluation of similarity of $r_{j,k}^{(\beta_m)}$ is based on p-values, while the rejection rate is performed based on significance level $\alpha = 0.05$. The rejection rate can be expressed as,

$$R(k) = \frac{\mathbb{P}\left(\text{reject } \mathcal{H}_{0,k} | r_{j,k}^{(\beta_m)}\right)}{\mathbb{P}\left(\text{accept } \mathcal{H}_{0,k} | r_{j,k}^{(\beta_m)}\right) + \mathbb{P}\left(\text{reject } \mathcal{H}_{0,k} | r_{j,k}^{(\beta_m)}\right)} \tag{8}$$

that is calculated for each value of Δd denoted with k.

III. Simulation Results

This section presents simulations results obtained with ray-tracing [10] and 3GPP 3D model [8, 15]. We consider an urban environment, i.e., 3D-UMa in [8] and separately investigate line-of-sight (LOS) and non line-of-sight (NLOS) propagation conditions. The carrier frequency is set to 3.5 GHz, while an omni-directional antenna pattern is considered in both cases, at the transmitter and receiver. In order to have a fair comparison between the two models, the geometry of the model is kept fixed, i.e., the positions of transmitter and receive locations and their corresponding heights. Specifically for the 3D-UMa, we use the values of 25 m for base station height and 1.5 m for the user height, as recommended in 3GPP TR36873. In the case of the 3GPP 3D channel model 500 simulation realizations are considered, whereas for the ray-tracing 90 different realizations. Each realization in the ray-tracing simulator comprises a unique urban environment, as the one shown in Figure 1, in order to account for an ensemble average.

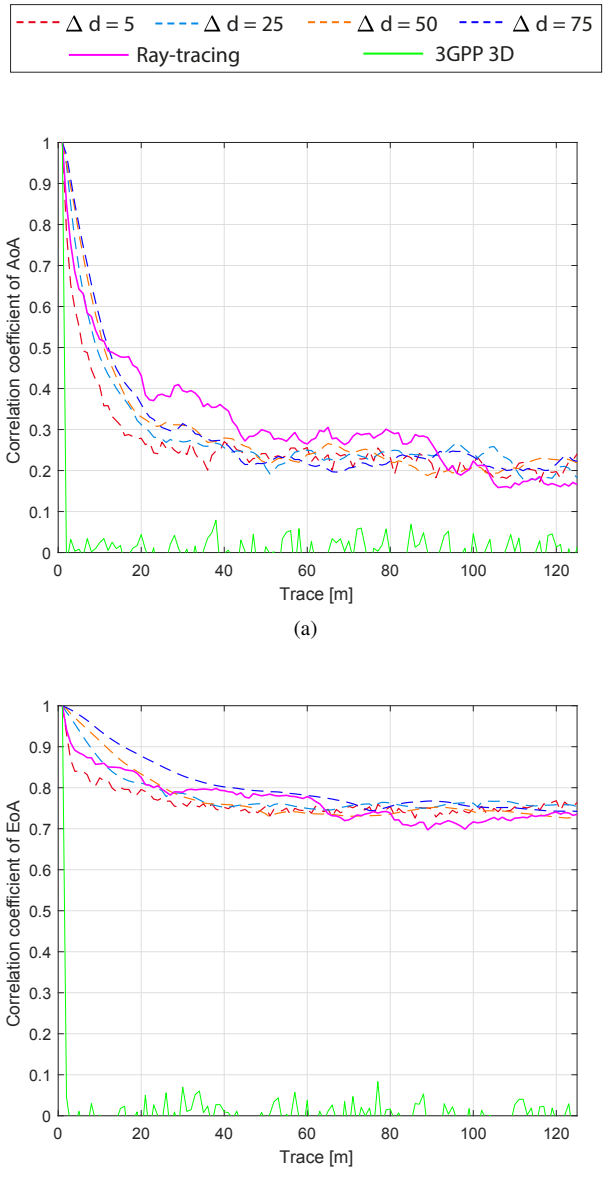

Fig. 3: Correlation coefficient of angles of arrival in LOS evaluated along the trace for ray-tracing, 3GPP 3D channel model without spatial consistency and 3GPP 3D channel model with spatial consistency modeled for different values of parameter Δd: (a) angle of arrival in azimuth and (b) angle of arrival in elevation.

A. Validation of the spatial consistency model

Based on (1), the correlation coefficient is estimated for both AoA and EoA for consecutive spatial positions as explained in Section II-A. The trace of consecutive spatial positions is considered with a length of $J = 125$ m, where the initial position of the trace is always taken as a reference point when

calculating the correlation coefficient. Figure 3 shows the correlation coefficient for AoA and EoA considering the LOS propagation condition. Three different cases are evaluated: the 3GPP 3D channel model, the ray-tracing model and the 3GPP 3D channel model with spatial consistency from [7] with different values of Δd. As expected, the results reveal no

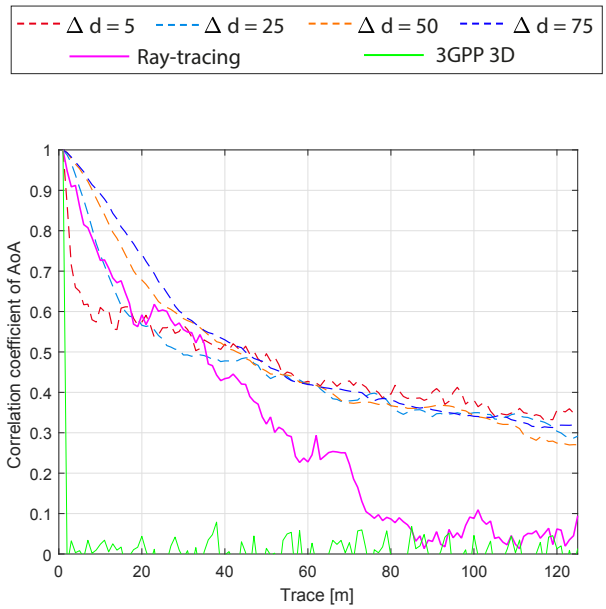

Fig. 4: Correlation coefficient of angles of arrival in NLOS evaluated along the trace for ray-tracing, 3GPP 3D channel model without spatial consistency and 3GPP 3D channel model with spatial consistency modeled for different values of parameter Δd: (a) angle of arrival in azimuth and (b) angle of arrival in elevation.

correlation in the case of the 3GPP 3D model, whereas we see a good agreement between the correlation coefficient obtained for different values of Δd and the output from ray-tracing for both AoA and EoA indicated in Figure 3a and Figure 3b,

TABLE I: Rejection rates for different values of decorrelation distance for AoA and EoA in LOS and NLOS.

	AoA		**EoA**	
	LOS	NLOS	LOS	NLOS
$\Delta d = 5$	0.0094	0.4417	**0.0167**	0.0667
$\Delta d = 10$	**0.0083**	0.3813	0.0333	**0.0083**
$\Delta d = 15$	0.0167	0.3583	0.0417	0.0250
$\Delta d = 20$	0.0238	**0.0250**	0.1917	0.0513
$\Delta d = 25$	0.0250	0.0258	0.1167	0.0833
$\Delta d = 35$	0.0417	0.3750	0.1250	0.1333
$\Delta d = 45$	0.0417	0.4083	0.2545	0.1833
$\Delta d = 60$	0.0583	0.5083	0.5083	0.3500

TABLE II: The parametric values of decorrelation distance based on lowest rejection rates for AoA and EoA in LOS and NLOS.

	LOS	**NLOS**
AoA	$\Delta d = 10$	$\Delta d = 20$
EoA	$\Delta d = 5$	$\Delta d = 10$

respectively. Comparing these two cases, we notice a lower correlation coefficient for AoA. This is reasonable since the angles in elevation are more confined in space than the angles in azimuth.

The correlation coefficient for the NLOS propagation condition is shown in Figure 4. Similar to the LOS case, the 3GPP 3D channel model shows no correlation. The results in terms of correlation coefficient for different values of Δd are in good agreement especially for the spatial positions in proximity to the initial position, up to around $50\,\mathrm{m}$, for both AoA and EoA. Overall, in the case of EoA, the behaviour from ray-tracing is close to the behaviour evaluated for different values of Δd, as indicated in Figure 4b.

B. Parametrization of the spatial consistency model

In order to find the value of Δd that is significantly closest to the correlation coefficient produced by ray-tracing we employ the hypothesis testing as described in Section II-B. Considering the correlation coefficient values for each spatial position along the trace, the corresponding rejection rates are calculated based on (8). Table I shows the rejection rates for all considered cases, AoA and EoA in LOS and NLOS.

Finally, the parametric values of Δd that give the lowest rejection rate are summarized in Table II. Intuitively, in order to achieve the spatial correlation observed with ray-tracing simulation, a higher value of Δd is necessary for the NLOS case compared to LOS.

IV. Future Work

The focus of this work is to first validate the model for spatial consistency. We only considered the 3GPP 3D channel model at carrier frequency of $3.5\,\mathrm{GHz}$, however our model can be applied to all types of GSC that are currently standardized,

including channel models for millimeter wave band. As a future work, we will provide a full model of spatial consistency parametrized for various carrier frequencies covering different scenarios.

V. Conclusion

In this paper we investigate the spatial consistency of the 3GPP 3D channel model, considering our previously published model for spatial consistency. To have an understanding on spatial correlation for arrival angles over consecutive spatial positions, we perform ray-tracing simulations. In this work we show results specifically for angles of arrival in azimuth and elevation. Considering as a statistical measure the circular correlation coefficient we show that our model for spatial consistency is in good agreement with the behaviour reflected from ray-tracing. Next, we perform a binary hypothesis test in order to parametrize the decorrleation distance, used as an input parameter in our model. The parametric values for decorrelation distance are extracted for AoA and EoA individually for LOS and NLOS propagation conditions.

References

[1] E. Bjrnson, J. Hoydis, and L. Sanguinetti, "Massive MIMO Networks: Spectral, Energy, and Hardware Efficiency," *Foundations and Trends in Signal Processing*, vol. 11, no. 3-4, pp. 154–655, 2017. [Online]. Available: http://dx.doi.org/10.1561/2000000093

[2] T. L. Marzeta, *Fundamentals of Masive MIMO*, 1st ed. Cambridge University Press, Nov. 2016.

[3] F. Ademaj, M. Taranetz, and M. Rupp, "3GPP 3D MIMO Channel Model: A holistic implementation guideline for open source simulation tools," *EURASIP Journal on Wireless Communications and Networking*, 2016.

[4] L. Liu, C. Oestges, J. Poutanen, K. Haneda, P. Vainikainen, F. Quitin, F. Tufvesson, and P. D. Doncker, "The cost 2100 mimo channel model," *IEEE Wireless Communications*, vol. 19, no. 6, pp. 92–99, December 2012.

[5] WINNER II WP1, "WINNER II channel models," *IST-4-027756 WINNER II Deliverable D1.1.2*, Sept. 2007.

[6] S. Jaeckel, L. Raschkowski, K. Brner, and L. Thiele, "QuaDRiGa: A 3-D Multi-Cell Channel Model With Time Evolution for Enabling Virtual Field Trials," *IEEE Transactions on Antennas and Propagation*, vol. 62, no. 6, pp. 3242–3256, June 2014.

[7] F. Ademaj, M. K. Mueller, S. Schwarz, and M. Rupp, "Modeling of Spatially Correlated Geometry-Based Stochastic Channels," in *2017 IEEE 86th Vehicular Technology Conference (VTC-Fall)*, Sept 2017, pp. 1–6.

[8] 3rd Generation Partnership Project (3GPP), "Study on 3D channel model for LTE," 3rd Generation Partnership Project (3GPP), TR 36.873, Sept. 2014.

[9] ——, "Study on channel model for frequencies from 0.5 to 100GHz," 3rd Generation Partnership Project (3GPP), TR 38.901, Dec. 2017.

[10] K. Guan, X. Lin, D. He, B. Ai, Z. Zhong, Z. Zhao, D. Miao, H. Guan, and T. Kürner, "Scenario modules and ray-tracing simulations of millimeter wave and terahertz channels for smart rail mobility," in *2017 11th European Conference on Antennas and Propagation (EUCAP)*, March 2017, pp. 113–117.

[11] D. He, B. Ai, K. Guan, Z. Zhong, B. Hui, J. Kim, H. Chung, and I. Kim, "Channel measurement, simulation, and analysis for high-speed railway communications in 5g millimeter-wave band," *IEEE Transactions on Intelligent Transportation Systems*, pp. 1–15, 2017.

[12] K. Guan, G. Li, D. He, L. Wang, B. Ai, R. He, Z. Zhong, L. Tian, and J. Dou, "Spatial consistency of dominant components between ray-tracing and stochastic modeling in 3gpp high-speed train scenarios," in *2017 11th European Conference on Antennas and Propagation (EUCAP)*, March 2017, pp. 3182–3186.

[13] N. Fisher and A. J. LEE, "A correlation coefficient for circular data," vol. 70, 08 1983.

[14] R. Fisher, "Frequency Distribution of the Values of the Correlation Coefficient in Samples from an Indefinitely Large Population," *Biometrika*, vol. 10, no. 4, pp. 507–521, May 1915.

[15] F. Ademaj, M. Taranetz, and M. Rupp, "Implementation, validation and application of the 3GPP 3D MIMO channel model in open source simulation tools," in *2015 International Symposium on Wireless Communication Systems (ISWCS)*, Aug 2015, pp. 721–725.